ELSEVIER

Surface Science 448 (2000) L207–L212

surface science

www.elsevier.nl/locate/susc

Surface Science Letters

Surface structure of ultra-thin $A1_2O_3$ films on metal substrates

Myoung Bok Lee [a,*], Jung Hee Lee [a], Brian G. Frederick [b],
Neville V. Richardson [c]

[a] School of Electronic and Electrical Engineering, Kyungpook National University, Taegu, 702-701 South Korea
[b] Department of Chemistry, University of Maine, Orono, ME 04469, USA
[c] School of Chemistry, University of St. Andrews, St. Andrews KY16 9ST, UK

Received 23 August 1999; accepted for publication 29 December 1999

Abstract

The surface structure of ultra-thin Al_2O_3 films on NiAl(110) and Ru(0001) was investigated by using high-resolution electron energy loss spectroscopy (HREELS). On a semi-empirical basis, the three phonon loss features, ν_1 ($380 \sim 430$ cm^{-1}), ν_2 ($620 \sim 660$ cm^{-1}), and ν_3 ($850 \sim 900$ cm^{-1}), of crystalline Al_2O_3 films were assigned to collective excitations of the microscopic vertical stretching motion of in-phase O–Al layers and to the stretching motions of the tetrahedrally and octahedrally coordinated Al–O species, respectively. To a good approximation, the distinct observation of the ν_1 mode in the HREEL spectra of Al_2O_3 films can be a sign for the synthesis of a vertically well-defined Al_2O_3 phase. The relative intensity between the ν_2 and the ν_3 loss features has been used to determine the most probable oxide structure, amorphous, transition, or α-like, by using the relative site occupation ratio of Al^{3+}cations to hexagonal closely packed O^{2-} anions. © 2000 Published by Elsevier Science B.V. All rights reserved.

Keywords: Aluminum oxide; Crystallization; Electron energy loss spectroscopy (EELS); Oxidation; Ruthenium; Surface structure, morphology, roughness and topography

1. Introduction

Heat treatment of boehmite (ν-AlOOH) in air has produced a series of transition aluminas, such as ν-, δ- and θ-, before final conversion to the most stable, anisotropic α-phase Al_2O_3 [1]: tetrahedrally coordinated Al^{3+}cations in the amorphous phase, both tetrahedrally and octahedrally coordinated Al^{3+}cations in the transition phase, and octahedrally coordinated Al^{3+}cations in the α-phase. The structural differences between the various phases mainly result from the alternative arrangements of Al^{3+}cations in the tetrahedral and the octahedral vacancies of the cubic closely packed and/or hexagonal closely packed oxygen arrays. In most transition bulk phases [1], the Al^{3+}cations are known to occupy both octahedral and tetrahedral sites, but the relative occupation ratios are largely unknown. It was an even more complicated job to correctly assign the phase of ultra-thin aluminium oxide films due in part to the structural differences between thin-film and known bulk-crystal structures [2] and in part to the unreleased strain in the thin films [3].

High-resolution electron energy loss (HREEL)

---

* Corresponding author. Fax: +82-53-950-5505.
E-mail address: mblee@ee.kyungpook.ac.kr (M.B. Lee)

PII: S0039-6028(00)00041-8

spectra of thin alumina films on metal substrates show commonly three distinct phonon features near the loss energies of $380 \sim 430\ \mathrm{cm}^{-1}$ (ν_1), $620 \sim 660\ \mathrm{cm}^{-1}$ (ν_2), and $850 \sim 900\ \mathrm{cm}^{-1}$ (ν_3) with slightly different relative loss intensities between the modes [4–9]. From the very initial oxidation of single-crystal Al(111) and parameterized lattice dynamical calculations, Erskine and Strong [10] and Strong et al. [4] first proposed that the ν_1, ν_2, and ν_3 modes originated from the out-of-phase motion between the in-phase surface and subsurface Al–O layers (ν_1), the out-of-phase motion of the surface Al–O species (ν_2), and the subsurface Al–O species (ν_3). However, Chen et al. [6] questioned this structural assignment for the ν_1 mode, indicating that it was relevant to incomplete oxidation of the ultra-thin Al films deposited on Mo(110). Furthermore, Frederick et al. [7] reported that rather than being due to incomplete oxidation of Al species, the mode was due to an extraordinary dipole-activity enhancement of the dipole inactive FK modes near the point, which was expected, especially in strained ultra-thin films on metal substrates [3]. Thus, the preparation of long-range-ordered alumina films seems a prerequisite for deriving a reliable vibrational model and for identifying defective oxide surfaces in many practical applications.

In this study, we have prepared a series of fully oxidized, crystalline Al_2O_3 film, in the thickness range of 5–30 Å on NiAl(110) substrate. In order to test the effects of the metallic Al-species, we also prepared ultra-thin crystalline Al_2O_3 films of about 5–30 Å on Ru(0001) and further annealed them in an ultra-high vacuum (UHV) for complete oxidation and better crystallinity. We propose an idea for the reliable determination of an oxide phase using the relative intensity ratio between the three typical phonon features of the ultra-thin Al_2O_3 films.

2. Experimental

This investigation was carried out in a two-level, stainless-steel, UHV apparatus with surface preparation facilities and many in-situ characterization tools, such as low-energy electron diffraction (LEED), Auger electron spectroscopy (AES), X-ray photoelectron spectroscopy (XPS), temperature-programmed desorption (TPD), and HREELS. A rotatable, single-stage hemispherical analyzer (VSW HA50) was equipped for the angular-dependent AES, XPS, and HREELS experiments with an electron-gun source (VSW EG5), a twin anode, a non-monochromatized X-ray source (PSP TA10), and a fixed, single-stage electron monochromator (VSW monochromator), respectively. Most vibrational EEL spectra were collected in a specular direction at a scattering angle of 45° with respect to the surface normal and at incident beam energies of 4–30 eV. Most of the measurements were made near 300 K at a background pressure in the $1–3 \times 10^{-10}$ mbar range. The typical resolutions (full width at half maximum) of the elastic peak in the HREEL spectrum were $60–70\ \mathrm{cm}^{-1}$ for a well-ordered alumina surface.

3. Results and discussion

Fig. 1 shows HREEL spectra obtained from NiAl(110) samples with 200 and 2000 L O_2 exposures near room temperature and from NiAl(110) samples exposed to 2000 L of oxygen and subsequently annealed at 600 and 1300 K in UHV. With increasing oxygen exposure, several new phonon bands appeared in the low-frequency regime, and a very similar vibrational spectrum was also reported for low doses of oxygen on Al(111) single-crystals [4,5,10]. These phonon bands can be properly assigned to the deformative, symmetric, and asymmetric stretching motions of surface AlO_x clusters rather than to a structured Al_2O_3 film [11]. On this basis, it would be unreliable to find a close relationship between the phonon bands of surface AlO_x clusters and those of structured Al_2O_3 thin films. Final annealing at 1300 K in UHV resulted in a long-range, well-ordered aluminium-oxide thin film with a thickness of about 5 Å and the corresponding HREEL spectrum illustrated three, symmetric phonon bands, ν_1, ν_2, and ν_3 at 400, 630, and $870\ \mathrm{cm}^{-1}$, respectively, accompanied by three high-frequency modes at about 1270, 1485, and $1730\ \mathrm{cm}^{-1}$.

Thicker overlayers on NiAl(110) with thick-

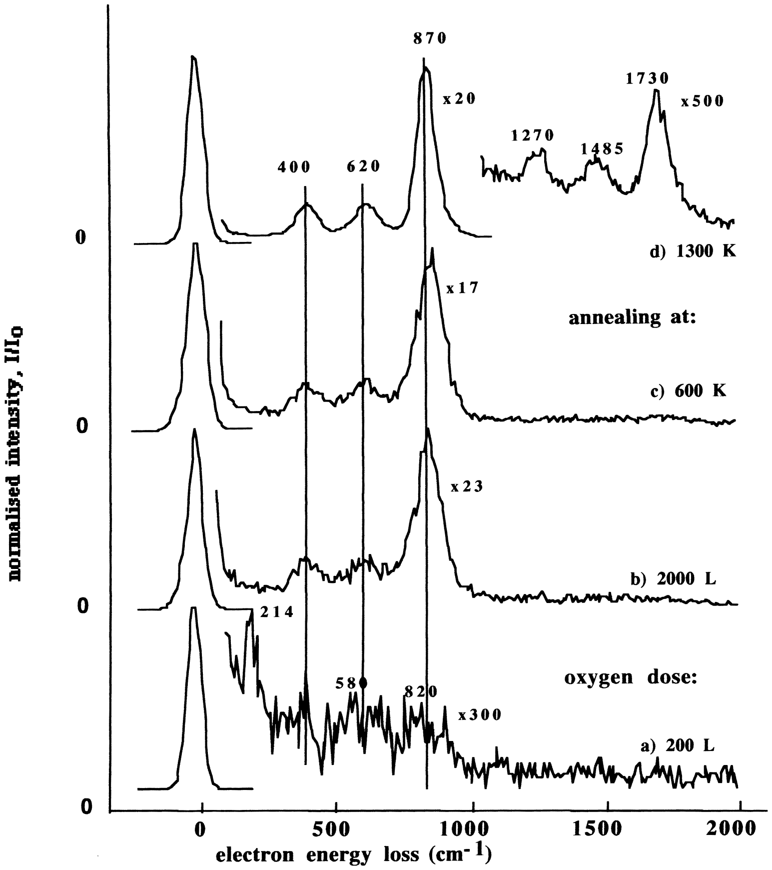

Fig. 1. HREEL spectra from the NiAl(110) surfaces: (a) 200 L and (b) 2000 L O_2 exposure at 300 K; annealed at (c) 600 K and at (d) 1300 K after a 2000 L O_2 exposure. $E_p = 5$ eV, and $\theta_i = 45°$.

nesses of 18, 25 and 30 Å also resulted in three similar phonon bands at loss energies of 390 (ν_1), (ν_2), and 890 (ν_3) cm^{-1}. The relative intensities of the three phonon modes with respect to the elastic peak were clearly different from those of the 5 Å film and increased quasi-linearly as the thickness of the oxide on NiAl(110) increased. In fact, the relative intensity of the highest-frequency mode at 10 eV was ~0.025 for 5 Å, ~0.111 for 18 Å, ~0.133 for 25 Å, and 0.196 for 30 Å. Almost the same phonon structures were obtained from the HREELS measurements on ultra-thin crystalline Al_2O_3 films on Ru(0001) substrates and with a thickness of about 5–30 Å, and the results are illustrated in Figs. 2 and 3. As shown, a fully oxidized Al_2O_3 film of about 5 Å on Ru(0001) reveals three well-resolved symmetric phonon features, at 430, 640, and 870 cm^{-1}, resembling the loss energies and the relative intensity ratios of the well-ordered 5 Å Al_2O_3 film on NiAl(110). Heavily oxidized 20–30 Å Al_2O_3 films deposited on Ru(0001) in O_2 or in an O_2/H_2O mixture also demonstrated the corresponding three phonon loss features at 380, 630, and 900 cm^{-1}, and further annealing resulted in only a slight enhancement of the signal-to-noise ratio. Details of the loss frequencies and the relative intensities are given in Table 1.

In a semi-empirical sense, a new origin can be suggested for each of the three main loss features in transition Al_2O_3 films consisting of both octahedral and tetrahedral Al^{3+}occupation. The ν_3 loss feature at 820~900 cm^{-1} is due to a group of microscopic stretching motions between the octahedrally coordinated Al^{3+}cation and its six near-

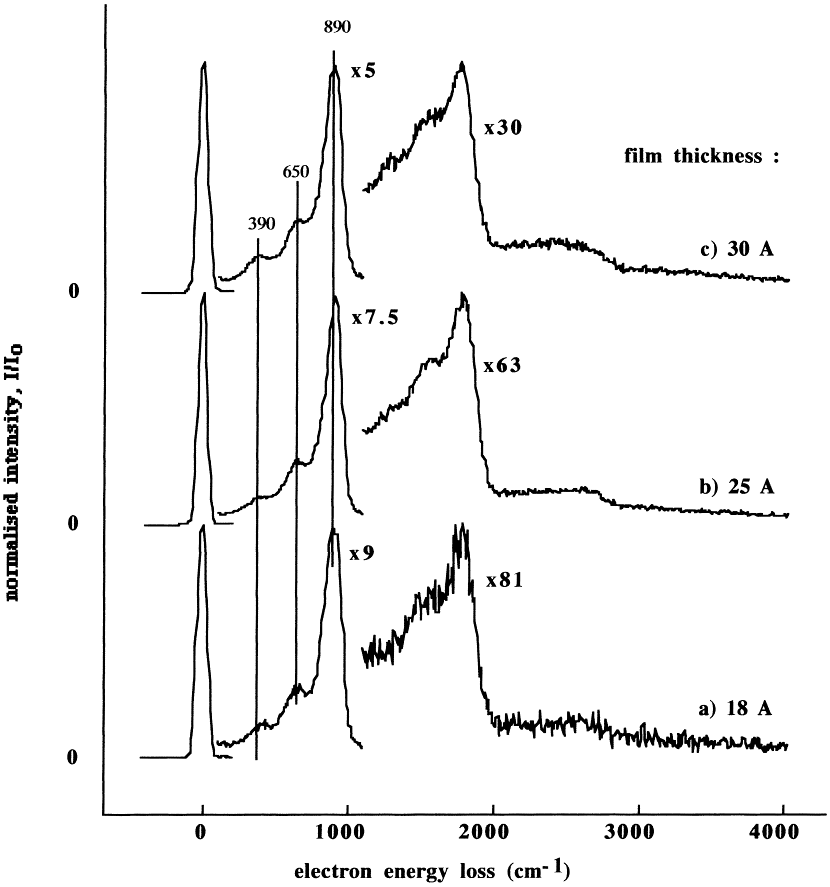

Fig. 2. HREEL spectra of thicker oxide films on NiAl(110) recorded at $E_p=10$ eV, $\theta_i=45°$: (a) 18, (b) 25, and (c) 30 Å.

est-neighbour O^{2-} anions, the ν_2 loss feature at $620\sim650\ \mathrm{cm}^{-1}$ is due to a group of stretching motions between the tetrahedrally coordinated Al^{3+}cation and its four nearest-neighbour O^{2-} anions, and the ν_1 loss feature at $380\sim430\ \mathrm{cm}^{-1}$ is due to a vertical stretching motion of the subsequent in-phase O–Al planes. Therefore, a clear observation of the ν_1 loss feature may be a sign for the synthesis of vertically well-defined crystalline Al_2O_3 films on NiAl(110) and Ru(0001), as shown in Figs. 1 and 3. The ν_1 loss mode may also indicate highly near-surface localized characteristics, such as less dispersive energy loss and relatively lower intensity, depending largely on the thin-film processing parameters of oxidation/annealing temperature and the metal substrates used. From both previous and present HREEL spectra of ultra-thin Al_2O_3 films, one can propose the feasibility of vertically well-layered Al_2O_3 films on Al(111) [4,5,10], Mo(110) [6], NiAl [8,9] and Ru(0001) [7]. Near-surface Al–O layers may determine the strengths of the dipole moments of the ν_1 mode so that the resultant intensity may be less sensitive to sample thickness changes from 5 to 24 Å on Ru(0001), as indicated in Fig. 3. Instead, long-range, well-ordered films on NiAl(110) show a systematic increase in relative intensity with increasing oxide thickness from 2 to 10 Al–O layers.

The population of the tetrahedral Al^{3+} sites in-phase alumina with a spinel structure is twice that of the octahedral Al^{3+} sites, and three slightly different sets of O–Al bonds exist in the octahedron AlO_6^{9-} cluster configuration and two values

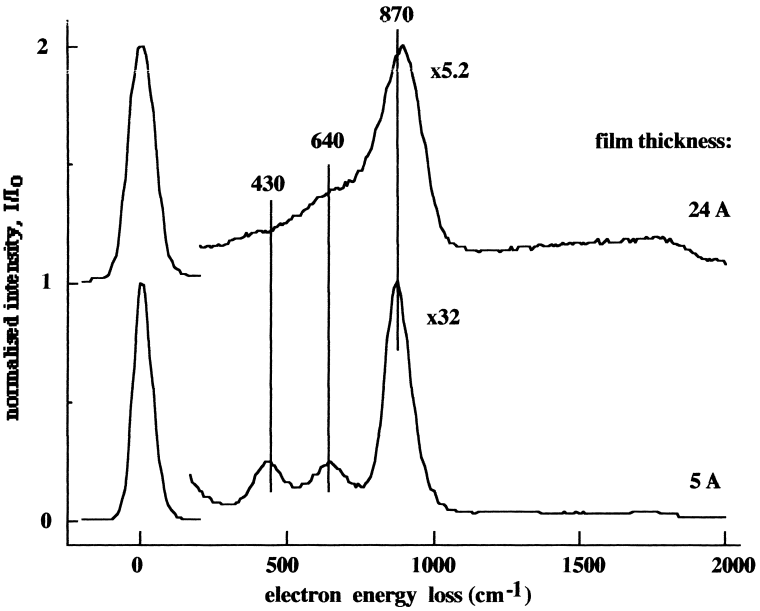

Fig. 3. HREEL spectra of crystalline 5 and 24 Å Al_2O_3 films on Ru(0001) recorded at $E_p = 10$ eV and $\theta_i = 45°$.

in the tetrahedron geometry [12]. Since the relative oscillator strength was totally unknown for octahedral and tetrahedral coordination, it was not easy to estimate the probable occupation ratio between the tetrahedral and the octahedral sites in most transition phases. However, now, using an occupation ratio of 1:2 between the tetrahedral and octahedral sites, especially for the ν-phase (most of tetrahedral sites will be unoccupied), one can roughly correlate the ratio $1(1\times4){:}3(2\times6)$ of the total microscopic Al–O oscillators between the tetrahedron and the octahedron geometries to the observed relative intensity ratio between the ν_2 and the ν_3 modes. Thus, this expected ratio of 0.33 between the tetrahedron and the octahedron geometries seems to be in good agreement with the observed intensity ratio of ~0.33 between the ν_2 and the ν_3 modes in thicker Al_2O_3 films on NiAl(110). The broadness of the ν_2 and the ν_3 loss features may be relevant to the existence of multi-oscillators with slightly different O–Al bond strengths in each cluster geometry. On this basis,

Table 1

Energies and relative intensities of the ν_1, ν_2, ν_3 single and $\nu_1+\nu_3$, $\nu_2+\nu_3$, $2\nu_3$ multiple loss events observed from ultra-thin Al_2O_3 films on metal substrates (mode unit: cm^{-1})

	ν_1 mode I_1/I_0	ν_2 mode I_2/I_0	ν_3 mode I_3/I_0	ν_{13} mode I_{13}/I_0	ν_{23} mode I_{23}/I_0	ν_{33} mode I_{33}/I_0
Al_2O_3 on Al(111)	430	645	865	1290	1510	1730
5A Al_2O_3 on Ru(0001)	430	640	880	1250	1460	1690
	0.008	0.008	0.32			
24A Al_2O_3 on Ru(0001)	374	639	900	1270	1485	1730
	0.008	0.017	0.063			
5A Al_2O_3 on NiAl(110)	400	620	870	1270	1485	1730
	0.0058	0.0055	0.027	0.000509	0.000412	0.00057
30A Al_2O_3 NiAl(110)	387	653	887	1258	1540	1758
	0.0336	0.065	0.196	0.0194	0.0266	0.0334

the most probable structure of the 18–30 Å Al_2O_3 films prepared on NiAl(110) would be a ν-like transition phase with an Al^{3+}occupation ratio of 1:2 between the tetrahedral and the octahedral sites of the cubic/hexagonal closely packed oxygen arrays.

The 5 Å film on NiAl(110) can be proposed to have a specific structure with a 3.3 times higher Al^{3+} occupation of octahedral sites with respect to the tetrahedral sites since the observed intensity ratio was 0.20 between the ν_2 and the ν_3 modes. A similar discussion is possible for samples on Ru(0001), and the analysis results in an occupation ratio of 1:2.7 for the 5 Å film and 1:2.5 for the 24 Å film since their observed intensity ratios between the ν_2 and the ν_3 modes were 0.25 and 0.27, respectively. Therefore, the considerably enhanced Al^{3+} occupation of the octahedral sites with respect to the tetrahedral sites may reflect electronic, vibrational, and structural characteristics of an α-like Al_2O_3 phase, but from the presence of the ν_2 and the ν_3 modes in HREEL spectra, most of the previously reported oxide films on metal substrates can be suggested to have transition phases/structures with slightly different Al^{3+} occupation ratios between the tetrahedral and the octahedral sites of the cubic/hexagonal closely packed oxygen arrays.

4. Conclusions

The HREEL spectra were newly analyzed to determine the most probable structure by using the three typical phonon loss features of the crystalline Al_2O_3 films, ν_1 ($380\sim430\ \mathrm{cm}^{-1}$), ν_2 ($620\sim660\ \mathrm{cm}^{-1}$), and ν_3 ($850\sim900\ \mathrm{cm}^{-1}$). New origins for the ν_1, the ν_2, and the ν_3 loss features were proposed as being collective excitations of a vertical stretching motion of the subsequent in-phase O–Al planes and a group of microscopic stretching motions between the octahedrally and tetrahedrally coordinated Al–O species in transition Al_2O_3 film, respectively. Thus, the observation of an intense ν_1 loss feature can be a sign for the synthesis of vertically well-defined crystalline Al_2O_3 films on metal substrates.

In conclusion, the considerably enhanced Al^{3+} occupation of the octahedral sites with respect to the tetrahedral sites may reflect electronic, vibrational, and structural characteristics of an α-like Al_2O_3 phase, but from the presence of the ν_2 and the ν_3 modes in HREEL spectra, most of the previously reported oxide films on metal substrates can be suggested as having transition phases/structures with slightly different Al^{3+} occupation ratios between the tetrahedral and the octahedral sites of the cubic/hexagonal closely packed oxygen arrays. Reliable lattice-dynamical modeling based on the proposed microscopic oxide structures would be a great help for further detailed explanations of both the behaviors of the three loss features and the relevant electronic, optical, and structural characteristics of ultra-thin crystalline Al_2O_3 films on metal substrates.

Acknowledgements

Dr. M. B. Lee wishes to acknowledge the invaluable technical support and advice by reseach staff during his study at the surface Science Research Centre of Liverpool University in the United Kingdom.

References

[1] S.J. Wilson, J.D.C. McConnel, J. Solid State Chem. 34 (1980) 315.

[2] P.A. Thiry, M. Liehr, J.J. Pireaux, R. Sporken, R. Caudano, J.P. Vigneron, A.A. Lucas, J. Vac. Sci. Technol. B 3 (1985) 1118.

[3] M. Liehr, P.A. Thiry, J.J. Pireaux, R. Caudano, Phys. Rev. B 34 (1986) 7471.

[4] R.L. Strong, B. Firey, F.W. de Wette, J.L. Erskine, Phys. Rev. B 26 (1982) 3483.

[5] J.E. Crowell, J.G. Chen, J.J.T. Yates, Surf. Sci. 165 (1986) 37.

[6] P.J. Chen, M.L. Colaianni, J.J.T. Yates, Phys. Rev. B 41 (1990) 8025.

[7] B.G. Frederick, G. Apai, T.N. Rhodin, Phys. Rev. B 44 (1991) 1880.

[8] R.M. Jaeger, H. Kuhlenbeck, H.-J. Freund, M. Wuttig, W. Hoffman, R. Franchy, H. Ibach, Surf. Sci. 259 (1991) 235.

[9] P. Gassmann, R. Franchy, H. Ibach, Surf. Sci. 319 (1994) 95.

[10] J.L. Erskine, R.L. Strong, Phys. Rev. B 25 (1982) 5547.

[11] B.G. Frederick, M.B. Lee, N.V. Richardson, Surf. Sci. 348 (1996) L71.

[12] S. Thomas, P.M.A. Sherwood, Anal. Chem. 64 (1992) 2488.